

RSC Advances



This is an *Accepted Manuscript*, which has been through the Royal Society of Chemistry peer review process and has been accepted for publication.

Accepted Manuscripts are published online shortly after acceptance, before technical editing, formatting and proof reading. Using this free service, authors can make their results available to the community, in citable form, before we publish the edited article. This *Accepted Manuscript* will be replaced by the edited, formatted and paginated article as soon as this is available.

You can find more information about *Accepted Manuscripts* in the [Information for Authors](#).

Please note that technical editing may introduce minor changes to the text and/or graphics, which may alter content. The journal's standard [Terms & Conditions](#) and the [Ethical guidelines](#) still apply. In no event shall the Royal Society of Chemistry be held responsible for any errors or omissions in this *Accepted Manuscript* or any consequences arising from the use of any information it contains.

**Simultaneous determination of Ciprofloxacin and Paracetamol by Adsorptive Stripping
Voltammetry using Copper Zinc Ferrite nanoparticles modified carbon paste electrode**

Mal Phebe Kingsley, Pramod K. Kalambate, Ashwini K. Srivastava*

Department of Chemistry, University of Mumbai, Vidyanagari, Santacruz (E),
Mumbai-400098, India.

***Corresponding Author:** Tel.: +91 22 26527956; Fax: +91 22 26528547.

Email: aksrivastava@chem.mu.ac.in, akschbu@yahoo.com

ABSTRACT

This work presents the development of an electrochemical sensor in the form of a copper zinc ferrite nanoparticles modified carbon paste electrode (CZF-CME) for the simultaneous determination of ciprofloxacin (CIP) and paracetamol (PA) using adsorptive stripping differential pulse voltammetry. The results indicate that the modified electrode exhibited enhancement of the oxidation peak current and shift in the oxidation potential to lower values in comparison with plain carbon paste electrode (CPE) for ciprofloxacin and paracetamol. The electrochemical performances of the modified electrode were investigated by cyclic voltammetry, chronocoulometry and electrochemical impedance spectroscopy, indicating the greater affinity of CIP and PA at the CZF-CME than at PCPE. Under the optimized conditions, the linear working ranges are from 9.09×10^{-7} M to 4.70×10^{-3} M and 1.85×10^{-7} M to 4.76×10^{-4} M for CIP and PA respectively. The detection limits (S/N=3) of 2.58×10^{-9} M and 8.85×10^{-8} M for CIP and PA respectively were obtained when taken together. The CZF-CME showed relatively high sensitivity, selectivity, stability and the proposed method was successfully used for individual and simultaneous determination of ciprofloxacin and paracetamol in pharmaceutical formulations, serum and urine samples.

Keywords: Ciprofloxacin, Paracetamol, Copper Zinc Ferrite nanoparticles, Modified carbon paste electrode, Adsorptive Stripping Differential Pulse Voltammetry.

1. INTRODUCTION:

Fluoroquinolones are important antibacterial group of drugs which have been widely used for treatment of many bacterial infections. Ciprofloxacin (1-cyclopropyl-6-fluoro-1, 4 dihydro-4-oxo-7-(1-piperaziny)-3-quinolinecarboxylic acid) is a second generation fluoroquinolone.¹ It is a broad-spectrum antibiotic, active against both Gram-positive and Gram negative bacteria. It is used for the treatment of urinary and lower respiratory tract infections, anthrax, urethral and cervical gonococcal infections, bone and joint infections, gastroenteritis, typhoid fever and acute sinusitis. It has excellent tissue penetration and available in both oral and intravenous formulations.² Over the years, a wide range of techniques have been used for the determination of ciprofloxacin such as high-performance liquid chromatography,³⁻⁵ micellar liquid chromatography,⁶ turbidimetry,⁷ spectrophotometry,⁸⁻¹⁰ spectrofluorometry,^{11,12} capillary electrophoresis^{13,14} and electrochemical analysis.¹⁵⁻¹⁹

Paracetamol (N-acetyl-p-aminophenol) is an analgesic and an antipyretic.²⁰ It is the most widely used over-the-counter analgesic agent in the world. It is the single most commonly taken drug in overdoses for deliberate self-poisoning, inducing life-threatening hepatic and renal failure.²¹ Varieties of methods have been used for the determination of paracetamol in pharmaceutical preparations and human plasma e.g. flow injection chemiluminescence,²² TLC densitometry,²³ RP-HPLC,²⁴ HPTLC,²⁵ capillary electrophoresis,²⁶ spectrophotometry²⁷ and electrochemical method.²⁸⁻³²

It is interesting to note, in-vitro and in-vivo studies have suggested that synergistic effect is produced when antibiotics are given in combination with antipyretic drug.³³ Thus combination of non-antibiotic drugs with antibiotics offers an opportunity to sample a previously untapped expanse of bioactive chemical space. Therefore, antipyretic medicaments in medical treatments with antibiotics are recommended.^{34, 35} As of now, even though antibiotic and antipyretic drugs are co-administered in therapeutic treatment, they are not commonly found in combination in pharmaceutical formulations. However, an antipyretic with antihistaminic and anti-

allergic formulations are available. Notwithstanding, in view of synergism produced as combinational formulations of antibiotic and antipyretic it is necessary therefore to develop an analytical method for simultaneous determination of these in order to detect any interference when present in combinations. Techniques like capillary electrophoresis, extractive spectrophotometry, HPLC and photo induced spectro-fluorimetry³⁶⁻³⁸ have been employed for simultaneous determination of its combined formulations in pharmaceutical and biological samples. However, its simultaneous determination by electrochemical technique has not been reported even though it has advantages like low cost, short analysis time and high sensitivity. Recently, electrochemical determination of drugs using modified electrode has received much attention because of its easier fabrication, selectivity and better reproducibility.^{39, 40} Nanomaterials modified carbon paste electrodes have also been widely used for simultaneous determination of different analytes^{41, 42} because of their exceptional properties such as high electrical conductivity, high surface area, mechanical strength and good chemical stability. Nanomaterials promote electron transfer reactions at the electrode surface when used as modifying material. Besides, metal oxide nanoparticles modified carbon paste electrode enhances the sensitivity of the electrode than plain carbon paste electrode.⁴³⁻⁴⁶ Ferrite nanoparticles due to their electrocatalytic activity and high surface area are commonly used as electrochemical sensors viz., magnetite nanoparticles⁴⁷ for simultaneous determination of ascorbic acid and folic acid, carbon nanotube decorated with nickel ferrite nanoparticles⁴⁸ for determination of sotalol and recently barium cobalt ferrite nanoparticles⁴⁹ for analysis of ciprofloxacin. The aim of this work is to first study the electrochemical behavior of ciprofloxacin and paracetamol and secondly to develop a highly sensitive electrochemical method for the simultaneous determination of ciprofloxacin (antibiotic) and paracetamol (antipyretic and analgesic) in pharmaceutical formulations, blood plasma and urine.

2. MATERIAL AND METHODS

2.1 Chemicals:

Chemicals used were of Analytical grade and used without any further purification. Graphite powder (amorphous graphite size, $<50\mu\text{m}$) and Paracetamol (PA) were purchased from S. D. fine Chemicals. Zinc ferrite, Magnetite, Copper ferrite, Copper zinc ferrite nanoparticles (with sizes $<100\text{nm}$) and Mineral oil were purchased from Sigma-Aldrich. Ciprofloxacin (CIP) was purchased from Fluka. A stock Britton–Robinson buffer (BR) solution 0.04 M with respect to boric, orthophosphoric and acetic acid was used to investigate pH dependence of CIP and PA. Other buffer solutions used were Acetate (Acet), Phosphate (Phos), Potassium hydrogen phthalate – Hydrochloric acid (KHP-HCl) and Citrate buffer (Cit). Double distilled water was used for the preparation of aqueous solutions. Few of the commercial pharmaceuticals of CIP and PA available from local pharmacies were subjected to analysis.

2.2. Instrumentation:

Electrochemical experiments have been performed on Eco Chemie, Electrochemical Work Station, model Autolab PGSTAT 30 using GPES software version 4.9005 and Frequency Response Analyser, software version 2.0. Electrode system employing an Ag/AgCl (3M KCl) as reference electrode, platinum electrode as counter electrode and a carbon paste working electrode (unmodified or modified) were used. ELICO LI 120 pH meter was used to measure the pH. Surface characterization of the copper zinc ferrite nanoparticles and composite of graphite-copper zinc ferrite nanoparticles was studied by scanning electron microscope (SEM) a FEI Inspect-250 model with an operating voltage of 20 kV.

2.3. Preparation of carbon paste electrode (CPE) and Copper zinc ferrite nanoparticles modified carbon paste electrode (CZF-CME):

The CPE was prepared by thoroughly mixing fine graphite powder with mineral oil at composition 70:30 (w/w -graphite/oil) using a motor and pestle and was allowed to homogenize for 48 hours.⁵⁰ CZF-CME was prepared by mixing mineral oil, graphite powder and copper zinc ferrite nanoparticles with various weight ratios. A portion of the paste was then packed into a Teflon micro tip (diameter 0.5mm) and a copper wire was inserted to establish an electrical contact. Electrode surface was smoothed on a zero grade butter paper to produce a reproducible working surface.

2.4. Voltammetric determination and SEM analyses

Cyclic voltammetric (CV) and adsorptive stripping differential pulse voltammetric (AdSDPV) studies were carried out for CIP and PA. Stock solution of CIP was prepared in 0.01M HCl and for paracetamol it was prepared in distilled water. An appropriate aliquot was taken in 25 mL standard volumetric flask and made up to the mark with 0.05 M KHP-HCl buffers (pH 3). The solution was then transferred into an electrochemical cell and the measurements were carried out at 25 ± 0.2 °C. Oxygen did not interfere in the measurements therefore N₂ gas purging was not required. The CV and AdSDPV studies were carried out by sweeping the potential between + 0.25 to +1.5 V and from + 0.2 to +1.4 V, respectively. The voltammograms were recorded using unmodified and modified (CZF-CME) carbon-paste electrodes. The EIS studies were performed on 5.00×10^{-5} M CIP or 1.00×10^{-6} M PA in 0.05M of KHP-HCl (pH 3) in the frequency range from 10^{-1} to 10^5 Hz at open circuit potential with amplitude of 5 mV. For SEM analysis, samples were sonicated in toluene and analyzed after drying the samples.

2.5. Treatment and determination of samples

The pharmaceutical preparations were Crocin and Calpol (Glaxo Smithkline Pharmaceuticals Ltd) each containing 500 mg of PA, Dolo 650 mg of PA (Micro labs Ltd), Flexon 650 mg of PA and 400 mg of Ibuprofen (Aristo Pharmaceuticals Pvt Ltd). Alcipro

(Alkem Laboratories Ltd) and Ciplox (Cipla) each contained 500 mg of CIP. Cibran (Ranbaxy Laboratories Ltd), Zoxan (FDC Ltd) and Cifran (Ranbaxy Laboratories Ltd), each contained 250 mg of CIP and Zoxan Eye/Ear drops -0.3% w/v (FDC Ltd).

2.5.1. Preparation of solution for individual determination of CIP or PA in tablets: Five tablets each were accurately weighed and finely powdered with a mortar and pestle. To the corresponding weight of the real sample 50 mL of 0.01M HCl was added. The mixture was shaken for 10 min and filtered through a Qualigens (615) filter paper made into a 100 mL volumetric flask. Appropriate volume of the sample was diluted to 25 mL with 0.05M KHP-HCl buffer (pH 3) and then transferred to an electrolytic cell for the determination of CIP or PA.

2.5.2. Preparation of solution for simultaneous determination of CIP and PA in tablets: Five tablets of CIP and PA each were accurately weighed and finely powdered separately with a mortar and pestle. A quantity equivalent to 500 mg /250 mg of ciprofloxacin and 500 mg / 650mg of paracetamol was accurately weighed, mixed and homogenized together. To the weighed mixture 50 mL of 0.01M HCl was added. Further, the procedure similar for individual drug determination was followed.

2.5.3. Preparation of solution for determination of CIP and PA in blood serum, urine and eye/ear drops: Urine and blood serum samples were obtained from local pathology laboratory and all ethical guidelines were followed in handling the samples for all measurements. To 0.5 mL of the blood serum / urine was taken in a 10 mL volumetric flask and made up with the supporting electrolyte in a cell and analyzed. 50 μ L of ear drops was added to 25 mL of supporting electrolyte in a cell and analyzed. Standard addition method was employed for quantification of CIP and PA in all pharmaceutical, blood serum and urine.

3. RESULTS AND DISCUSSION:

3.1. Scanning electron microscope (SEM):

The SEM image in Fig 1 shows the morphology of the CZF nanoparticles. Surface studies were done with SEM which confirms the formation of nano composite as shown in Fig.1. The SEM of Fig.1 (A) shows graphite particles, (B) shows spherical CZF nanoparticles and (C) the adsorption of CZF nanoparticles on graphite which attributes to the increase in surface area of the graphite - CZF composite. The chemical constituent of particles was analyzed by energy-dispersive X-ray spectrum for the CZF nanoparticles (Fig.1 (D)). It was observed that prominent peak appeared for Fe $L\alpha$ (0.705 keV), Cu $L\alpha$ (0.930 keV) and Zn $L\alpha$ (1.012 keV) indicating the presence of Iron, Copper and Zinc element present in the nanoparticles.

3.2. Effect of pH:

The effect of change in pH on peak potential for CIP and PA were investigated by differential pulse voltammetry from pH 2 to 10 with BR buffer. Standard solutions of CIP ($5.00 \times 10^{-5} \text{M}$) and PA ($1.00 \times 10^{-6} \text{M}$) were used to find the optimum pH of the supporting electrolyte at CPE. Fig.S1 (A) represents the plot of I_p vs. pH and E_p vs. pH for CIP and Fig. S1 (B) represents the plot of I_p (anodic) vs. pH and E_p (anodic) vs. pH for PA. The variation of anodic peak potential (E_p) with pH is linear for both the molecules. Increase in pH shifted the potential to less positive values suggesting the involvement of protons for the electro-oxidation of CIP and PA. A slope of -0.057V/pH and -0.050V/pH for CIP and PA respectively were observed, suggesting that same number of electrons and protons were involved for both the molecules. With the increase in pH the peak currents were found to increase in the beginning showing maximum at pH 3 and decrease thereafter for both the molecules. The reason could be due to the fact that the repulsive electrostatic interactions of the molecules with the surface of the electrode made the oxidation of CIP and PA at the electrode surface became kinetically less favorable. Therefore, pH 3 which showed maximum peak current for both the molecules was selected as the optimum pH for further studies. The effects of several supporting electrolytes (0.1M) viz., Acetate, Phosphate, Citrate and KHP-HCl buffer at pH 3

for 5.00×10^{-5} M CIP on peak current were tested (Fig. S2). Of these, KHP-HCl gave the best response in terms of peak height and the peak shape. Further, optimization of buffer concentration was carried out by varying KHP-HCl concentration in the range from 0.01M to 0.3M, the best peak response was observed for 0.05M of KHP-HCl (pH 3) and hence was used for further studies.

3.3. Effect of surface modification and Optimization of the amount of the modifier:

DPV study for 5.00×10^{-5} M CIP and 1.00×10^{-6} M PA in 0.05M of KHP-HCl (pH 3) at CPE and carbon paste electrodes modified with different nanoferrites viz., zinc ferrite, magnetite, copper ferrite and copper zinc ferrite (CZF-CME) were performed. It is observed from Fig. S3 that CZF-CME gave the best performance among the above mentioned ferrites and CPE in terms of peak current and resolution showing an increase in the electron transfer rate of CIP at the electrode surface. Similarly, paracetamol (data not shown) also gave a higher peak current at CZF-CME than that for unmodified carbon paste electrode and the other ferrite carbon paste modified electrodes taken. Considering the best response of CZF-CME over other ferrite based sensors it was therefore chosen for the entire work.

The effect of modifier on the oxidation of 5.00×10^{-5} M CIP and 1.00×10^{-6} M of PA has been shown in Fig.2 (A) and Fig. 2 (B), respectively at CPE and CZF-CME using cyclic voltammetry. The cyclic voltammograms of CIP shows an irreversible peak, whereas PA shows a well-defined quasi-reversible redox peaks at CPE and CZF-CME. It was observed from these figures that the modification of the CPE with CZF nanoparticles enlarged the peak current considerably by about 2.6 times for CIP and that for PA by 1.2 times with a decline in peak potential from 1.24 V to 1.16 V for CIP and from 0.61 V to 0.52 V for PA as compared to CPE. This indicates that the surface of the modified electrode has been significantly changed. CZF-CME provided an efficient interface and micro-environment for the electrochemical oxidation reaction of CIP and PA by increasing the electro-active surface area of the electrode.

The influence on the amount of CZF nanoparticles (Table S1) added to CPE was studied for CIP. The peak current increased with increase in the percentage weight of nanoparticles till the ratio of composition (w/w) for graphite: CZF nanoparticles: mineral oil was 60:10:30. There was a gradual decrease in peak current beyond this composition. This can be due to the increase in resistance of the CZF nanoparticles at the electrode to electron transfer. The surface area of CPE and CZF-CME having same nominal bore size were found to be 0.0212 cm^2 and 0.0434 cm^2 , respectively using the cyclic voltammogram of ferri/ferrocyanide system and Randles-Sevcik equation.⁵¹

3.4. Electrochemical Impedance Spectroscopy (EIS):

Electrochemical impedance spectroscopy was performed for $5.00 \times 10^{-5} \text{ M}$ CIP and $1.00 \times 10^{-6} \text{ M}$ PA in 0.05M of KHP-HCl (pH 3) to understand the electrochemical performance of CZF-CME over CPE. In the impedance measurement, the dc applied potential was held at an open circuit potential and a 5 mV amplitude ac potential was applied. 100 points per decade were acquired for the study. The voltage frequencies used for EIS measurements ranged from 100 kHz to 100 mHz. A suitable equivalent circuit known as Randles equivalent circuit is produced by the software to reflect the real electrochemical process and to enable a fit producing accurate value. This equivalent circuit is used to find out resistors and capacitors that pass current with same amplitude (inset in Fig.3) where 'Rs' is electrolyte resistance, 'R_{ch}' the charge transfer resistance, 'C_{dl}' the double layer capacitance and 'W' the Warburg impedance, in which charge-transfer resistance is in parallel with double layer capacitance.

The Nyquist plots for CIP and PA are shown in Fig. 3(A) and Fig. 3(B) respectively at the CPE and CZF-CME. It has two parts, a semicircular part and linear part. The semicircle represents the parallel combination of the R_{ct} and C_{dl}. It corresponds to the electron transfer limited process, and its diameter is equal to the electron transfer resistance. The greater the size of the semicircle greater the electron transfer resistance.⁵² The R_{ct} values obtained from Nyquist plots for $5.00 \times 10^{-5} \text{ M}$ CIP at CPE and CZF-CME from the EIS measurements was $645.58 \text{ } \Omega$ and

268.44 Ω respectively. Similarly, the charge transfer resistance value for 1.00×10^{-6} M PA at CPE and CZF-CME was found to be 367.23 Ω and 247.67 Ω . It is seen that CZF-CME electrode showed a smaller diameter when compared to that of the CPE for both the molecules. The measured data quality is of crucial importance for a reliable interpretation of impedance curves. Kramers-Kronig (K-K) relations are used to evaluate data quality which is true for EIS data to assess consistency and quality of measured impedance spectra. The K-K relations are integral equations which constrain the real and imaginary components of the impedance for systems that satisfy the conditions of causality linearity and stability. It has proven useful for confirming the self-consistency of electrochemical impedance data. The χ^2 provides the best fit for all experimental data points which satisfies the K-K relations. The test implied that the impedance data were validated with respect to impedances over a wide frequency range.⁵³ The K-K transformation gave a χ^2 for CIP and PA at CZF-CME as 1.292×10^{-2} and 1.6205×10^{-4} respectively and at CPE 1.443×10^{-1} and 6.33×10^{-2} respectively satisfying all the conditions for a good impedance data.

3.5. Cyclic Voltammetry:

The effect of scan rate were studied for 5.00×10^{-5} M CIP and 1.00×10^{-6} M PA for the purpose of investigating their reaction mechanism which are shown in Fig. 4(A) and Fig. 4 (B), respectively. The influence of scan rate was studied from 50 to 1000 mVs^{-1} for both the molecules at CZF-CME in 0.05M KHP-HCl (pH 3). The peak current varied linearly with increase in the scan rate for CIP (Fig.S4 (A)) with a regression equation

$$I_p = 0.007 v + 1.785 [R^2 = 0.992; I_p: \mu\text{A}, v: (\text{mV/s})] \quad (1)$$

validating a typical adsorption-controlled process. The peak potential shifted to more positive values with the increase of scan rate, which confirmed the irreversibility of the oxidation process (Fig.S4 (B)).

The effect of scan rate on the anodic and cathodic peak current of PA on CZF-CME shows a linear increase as the square root of scan rate increases (Fig S5(A)) indicating a diffusion controlled process with their respective linear regression equation as,

$$I_{pa} = 0.660 v^{1/2} - 0.662 \quad [R^2 = 0.997 \quad I_{pa}: \mu A, v^{1/2}: (mV/s)^{1/2}] \quad (2)$$

$$I_{pc} = -0.279 v^{1/2} - 0.181 \quad [R^2 = 0.995 \quad I_{pc}: \mu A, v^{1/2}: (mV/s)^{1/2}] \quad (3)$$

The oxidation peak potential is positively shifted and the reduction peak potential is negatively shifted (Fig S5 (B)). Also, plot of log (anodic peak current) versus log (scan rate), gave a straight line having a slope of 0.532 which is comparable with the theoretical slope of 0.5 for a diffusion controlled process and fulfilling the equation,

$$\log I_{pa} = 0.532 \log v - 0.291 \quad [R^2 = 0.997 \quad I_{pa}: \mu A, v: mVs^{-1}] \quad (4)$$

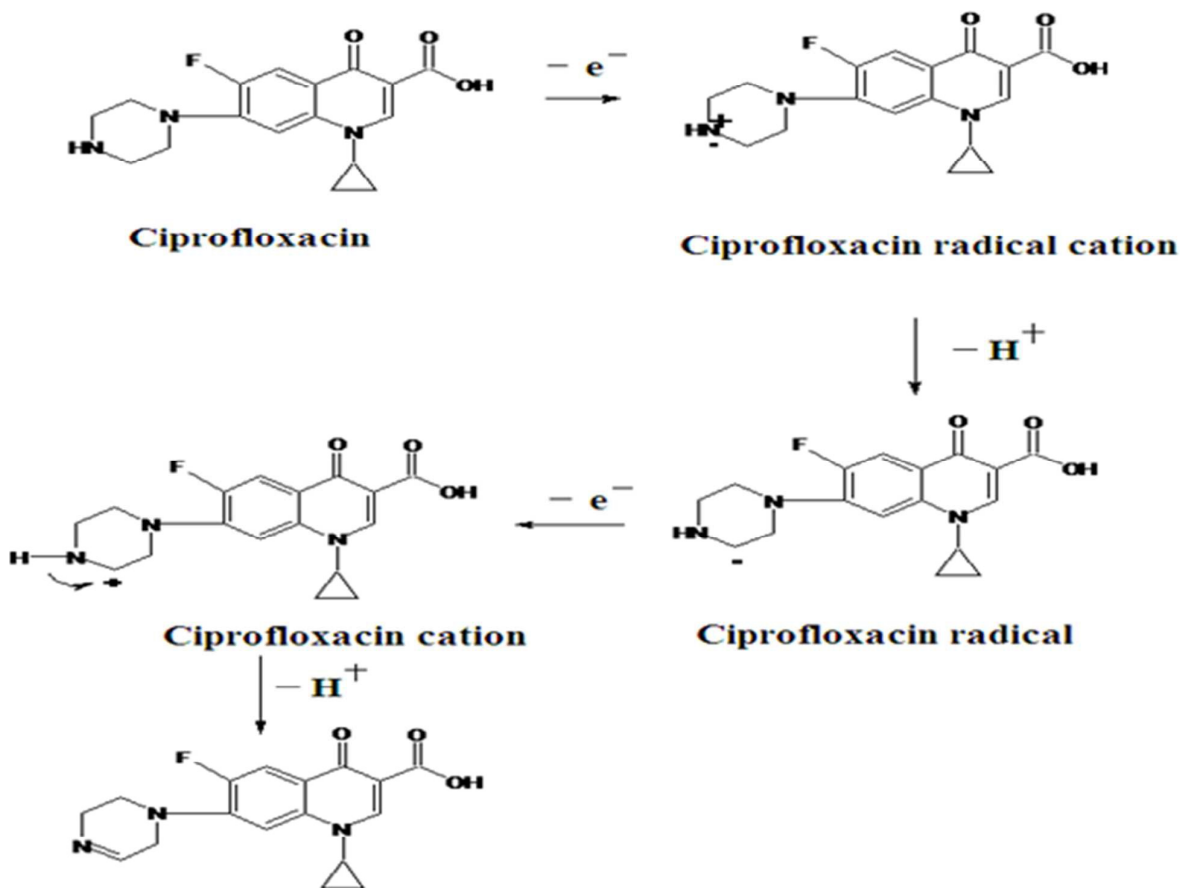
For a quasi-reversible or irreversible reaction the number of electrons (n) involved in the oxidation reaction was calculated from the following equation:⁵⁴

$$E_p - E_p/2 = 47.7/n\alpha \quad [mV \text{ at } 25^\circ C] \quad (5)$$

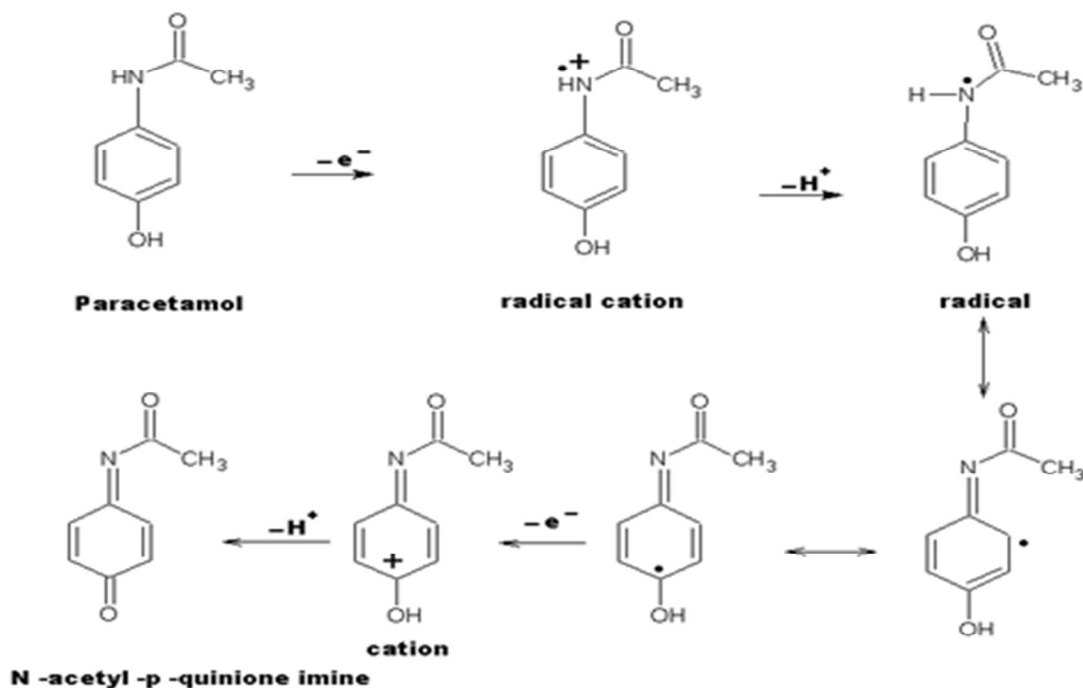
$E_p - E_p/2$ value for CIP and PA was found to be 50 mV and 40 mV respectively. On substitution in the above equation, assuming α as 0.5, ' n ' was calculated to be 1.91 for CIP and 2.3 for PA which indicated that two electrons were involved in the oxidation process of CIP and PA on the modified electrode. Since the oxidation occurred by transfer of the same number of electrons and protons for both the molecules therefore, two electrons and two protons transfer was involved in the electro-oxidation of CIP and PA at the CZF-CME. Scheme.1 (a) and 1(b) shows the electrochemical reaction process for the oxidation of CIP and PA at the CZF-CME respectively.

Scheme.1 (a) and (b) show the electrochemical reaction process for the oxidation of CIP and PA at the CZF-CME respectively. Both CIP and PA have a secondary amine group presenting a basic centre with the availability of non bonding electron as donor. Therefore, we presume that the first oxidation step takes place at $-NH$ group for both the molecules. For ciprofloxacin due to loss of two protons and two electrons the $-NH-CH_2-$ group is oxidized to

-N= CH- group. In case of paracetamol the radical cation formed at the -NH- group undergoes delocalization to give the product N-acetyl -p- quinone imine.⁵⁵



Scheme 1(a): Electro-oxidative mechanism of Ciprofloxacin



Scheme 1(b): Electro-oxidative mechanism of Paracetamol

3.6. Effect of accumulation parameters by Differential pulse voltammetry

3.6.1 Effect of accumulation potential and accumulation time

The dependence of differential pulse anodic stripping peak current for 5.00×10^{-5} M CIP on the accumulation potential from 0.5 V to 1.3 V were examined (Fig.S6 (A)). It was found that the maximum response was at 1.0 V and was an ideal choice for optimal sensitivity. The effect of accumulation time on the efficiency of drug onto the working electrode surface was evaluated over the time range from 0 *second* to 240 *seconds*. The resulting peak current accumulation time profile can be seen from the Fig.S6 (B). A steady enhancement in the peak current was observed over the range from 0 to 160 *seconds* and thereafter, the peak intensity gradually tended to a plateau. This could be probably indicating that the adsorption of CIP on CZF-CME surface has reached saturation. For practical purposes, the accumulation time was used as 160 *seconds* with an optimal stirring rate during the accumulation step which was found to be 800 *rpm*. The anodic and cathodic peak current were independent with variation in

potential (0.0 V to 1.4 V) and time (0 *second* to 240 *seconds*) for 1.00×10^{-6} M PA reconfirming that the process of PA reaching the CZF-CME surface was purely by diffusion.

3.6.2 Effect of potential sweep parameters:

Study was done on the effect of excitation pulse amplitude from 0.01V to 0.10V on the peak current for 5.00×10^{-5} M CIP. It was observed that the current increased as the pulse amplitude increased and the best peak shape was obtained at 60 mV pulse amplitude. After 60 mV, the shape of the peak was distorted. Therefore 60 mV pulse amplitude was the ideal choice for this operational parameter. The effect of scan rate on the peak current was studied over the range of 5–150 mVs^{-1} . As the scan rate was increased the peak current increased. Faster scan rates resulted in higher peak currents but background currents also increased. By taking peak current and background current into consideration the scan rate chosen was 100 mV s^{-1} .

3.7. Chronocoulometry (CC)

Double-potential step chronocoulometry was performed after point-by-point background subtraction for CIP and PA to evaluate the surface coverage of the electrode and the diffusion coefficient for both the molecules. According to the following equation⁵⁴

$$Q_t = (2nFD^{1/2} CA t^{1/2}) / \pi^{1/2} + nFA \Gamma^0 + Q_{dl} \quad (6)$$

Where, Q_t is the total charge in Coulombs, Q_{dl} is the double layer charging in Coulombs, n is the number of electrons, F is the Faradays constant (96485 C), C is the concentration in mol/cm^3 , A is the Area of the electrode (cm^2), t is time in seconds, Γ^0 is surface coverage in mol cm^{-2} and D is the Diffusion coefficient in $\text{cm}^2 \text{s}^{-1}$. The Anson plot of Q_t vs. $t^{1/2}$ showed a linear relationship for 5.00×10^{-5} M CIP and 1.00×10^{-6} M PA. From the slope of Anson plot, the diffusion coefficients (D) for CIP and PA can be estimated and from intercept the surface coverage (Γ^0) of the electrode is determined. Table 1 gives the calculated parameters. Increase in the value of charge due to adsorption at CZF–CME indicates greater accumulation of CIP

and PA on its surface rather than on CPE. The surface coverage of CIP and PA at CZF–CME is greater than for CPE indicating better response towards the modified electrode.

3.8. Determination of CIP and PA by Adsorptive Stripping Differential Pulse Voltammetry (AdSDPV):

CIP and PA were determined by AdSDPV technique (Table S2) individually and simultaneously. The linear working range (LWR), empirical limits of detection (LOD) (S/N=3), linear regression equation (LRE) and correlation coefficient (r) were determined and are shown in Table 2. Fig. 5(A) and Fig. 5(B) represents the voltammograms for separate determination of CIP and PA respectively.

There is no report on the simultaneous determination of CIP and PA by electrochemical technique. Therefore, the main objective of this study was to determine CIP and PA simultaneously using our proposed method. This was performed by simultaneously changing the concentrations of CIP and PA and recording their DPVs. To study their behavior, two separate sets of experiments were carried out. In the first instance, concentration CIP was increased in the presence of fixed concentrations of other (PA) and their voltammograms are given in Fig. 6(A) and vice versa as given in Fig. 6(B). For the second instance, both CIP and PA were determined by simultaneously increasing their concentrations as given in Fig. 6(C). From Table 2, it is observed that the LWR and LOD determined for CIP and PA simultaneously are in good agreement with when both were individually determined. Table 3 shows the comparison of the proposed sensor with the reported electrochemical sensors for the determination of CIP and PA individually. The comparative performance of the proposed sensor has lower detection limit and relatively large linear working range. Also, since it is a carbon paste electrode sensor the preparation of the electrode was easier and had good sensitivity as compared to other reported electrodes.

3.9. Validation studies, interference studies and analytical applications:

Five replicate measurements for 1.00×10^{-4} M CIP and 1.00×10^{-5} M PA over intra-day assay (single day, $n = 5$) and inter-day assay (for a period of 1 week) was performed for validation of the proposed method. Parameters such as repeatability, reproducibility, precision and accuracy of the analysis were obtained. Satisfactory bias and relative standard deviations (% RSD) were obtained and are presented in Table 4. The recoveries obtained confirmed high accuracy and the %RSD showed good precision of the proposed method.

Matrix effect on CIP and PA was determined by AdSDPV. The influences of peak current on interferents for both the molecules that are commonly present in biological media were investigated. Under optimized experimental conditions described above, the effects of some foreign species on the determination of CIP and PA at CZF-CME were evaluated. The peak current of 1.00×10^{-4} M CIP and 1.00×10^{-5} M PA showed no significant change even after the addition of 200-fold of Na^+ , K^+ , Mg^{2+} , Ca^{2+} , Cl^- , SO_4^{2-} , 150 -fold of glucose, uric acid and thiamine hydrochloride, 60 fold of caffeine, 10 fold of citric acid, 50 fold of 4 -aminophenol, 30 fold of aspirin, 30-fold concentration of lysine and 100 fold vitamin C showing that the present modified electrode was highly selective towards the determination of CIP and PA in the presence of common physiological interferents.

The validity of the CZF-CME was verified for the determination of CIP and PA in various pharmaceutical preparations by standard addition method. Amount of CIP and /or PA present in tablets are given in Table 5. The recovery of CIP and PA on the spiked samples (blood and urine) were determined and shown in Table S3 which ranged between 97.2% and 104.6% for CIP and 98.3% and 104.7% for PA indicating high reproducibility and reliability of the modified electrode.

4. CONCLUSION:

Interference free, rapid and simple operation of the proposed method using Copper Zinc Ferrite modified carbon paste electrode makes it suitable for the analysis of Ciprofloxacin

and Paracetamol simultaneously. The modified electrode has been used for determination of CIP and PA in tablets, urine and blood demonstrating the applicability of the method for real sample analysis. This sensor can be used for voltammetric determination of these analytes as low as 2.58 nM for CIP and 88.5 nM for PA with good reproducibility, sensitivity and reliability. The proposed method for the simultaneous determination of CIP and PA will offer a good alternative, both economically and environmentally, for quality control of pharmaceutical formulations in future.

Acknowledgement:

One of the authors (MPK) is grateful to the University Grants Commission, New Delhi, India for providing financial assistance under Faculty Improvement Programme for this work.

REFERENCES:

- [1] C. M. Oliphant, G. M. Green, *Am Fam Physician.*, 2002, **65**, 455–464.
- [2] D. M. Campoli-Richards, J. P. Monk, A. Price, P. Benfield, P. A. Todd, A. Ward, *Drugs.*, 1988, **35**, 373–447.
- [3] K. Marika, T. Kimiko, K. Tsutomu, N. Koichi, N. Shigeyuki, *Clin Chem.*, 1998, **44**, 1251–1255.
- [4] Z. Vybíralová, M. Nobilis, J. Zoulova, J. Květina, P. Petr, *J. Pharm. Biomed. Anal.*, 2005, **37**, 851–858.
- [5] N. M. Simon, T. Nahashon, K. Japhet, M. Alex, O. K. Gilbert, M. Kathryn, *J. Chromatogr. B.*, 2011, **879**, 146–152.
- [6] L. V. José, A. Lilia, P. Avismelsi, N. Alberto, *Anal. Chim. Acta.*, 2004, **516**, 135–140.
- [7] C. Edith, C. Laignier, R. Hérída, S. Nunes, *J. Pharm. Anal.*, 2013, **3**, 382–386.
- [8] F. Lorena, E. S. Elfrides, Schapoval, *Int. J. Pharm.*, 1996, **127**, 279–28.
- [9] S. N. Rajia, Yeakuty, J. Marzan, B. S. Kumar, *S. J. Pharm. Sci.*, 2011, **4**, 84–90.
- [10] M. I. Pascual-Reguera, P. G. Perez, M. D. Antonio, *Microchem. J.*, 2004, **77**, 79–84.
- [11] M. S. Attia, A. E. Amr, A. O. Youssef, *J. Photochem. Photobiol. A. Chemistry.*, 2012, **236**, 26–34.
- [12] N. Alberto, B. Oscar, B. Rosario, L. V. José, *Talanta.*, 2000, **52**, 845–852.
- [13] M. Katarzyna, P. Genowefa, T. Stefan, *J. Chromatogr. A.*, 2004, **1051**, 267–272.
- [14] Z. Xiaoming, D. Xing, D. Zhu, Y. Tang, L. Jia, *Talanta.*, 2008, **75**, 1300–1306.
- [15] A. A. J. Torriero, J. J. Juan, Ruiz-Díaz, S. Eloy, J. M. Eduardo, I. S. María, R. Julio, *Talanta.*, 2006, **69**, 691–699.
- [16] M. A. Abdalla, M. S. Salah, M. A. Al-Olyan, S. M. Al-Ghannam, *Talanta.*, 2003, **61**, 239–244.

- [17] Y. Ni, Y. Wang, S. Kokot, *Talanta.*, 2006, **69**, 216-225.
- [18] F. Lida, A. Mahnaz, *Colloids Surf. B.*, 2010, **81**, 110–114.
- [19] S. Zhang, S. Wei, *Bull. Korean Chem. Soc.*, 2007, **28**, 543-546.
- [20] A. Bertolini, A. Ferrari, A. Ottani, S. Guerzoni, R. Tacchi S. Leone, *CNS Drug Reviews.*, 2006, **12**, 250–275.
- [21] F. F. S. Daly, J. S. Fountain, L. Murray, A. Graudins, N. A Buckley, *Med. J. Aust.*, 2008, **188**, 296-302
- [22] W. Ruengsitagoon, S. Liawruangrath, A. Townshend, *Talanta.*, 2006, **69**, 976–983.
- [23] N. M. Mostafa, *J. Saudi Chem. Soc.*, 2010, **14**, 341–344.
- [24] M. Attimarad, *Pharm Methods.*, 2011, **2**, 61–66.
- [25] S. L. Borisagar, U. P. Jayswal, H. U. Patel, C. N. Patel, *Pharm Methods.*, 2011, **2**, 83–87.
- [26] F. Bohnenstengel, H. K. Kroemer, B. Sperker, *J. Chromatogr. B. Biomed. Sci. Appl.*, 1999, **721**, 295–299.
- [27] Sirajuddin , A. R. Khaskheli, A. Shah, M. I. Bhangar, A. Niaz, S. Mahesar, *Spectrochim Acta A.*, 2007, **68**, 747–751.
- [28] R. N. Goyal, S. P. Singh, *Electrochim. Acta.*, 2006, **51**, 3008–3012.
- [29] Bankim J. Sanghavi, Ashwini K. Srivastava, *Electrochim. Acta.*, 2010, **55**, 8638–8648.
- [30] A. R. Khaskheli, J. Fischer, J. Barek, V. Vyskocil, Sirajuddina, M. I. Bhangar, *Electrochim. Acta.*, 2013, **101**, 238–242.
- [31] A. T. E. Vilian, M. Rajkumar, S.M. Chen, *Colloids Surf. B. Biointerfaces.*, 2014, **115**, 295–301
- [32] Bankim J. Sanghavi, Ashwini K. *Anal. Chim. Acta.*, 2011, **706**, 246– 254.

- [33] G. Pasăre, V. Pasăre, N. Eftimescu, M. Ivan, *Zentralbl Bakteriol Naturwiss.*, 1979, **134**, 640-647.
- [34] K. Akilandeswari, K. Ruckmani, S. Abirami, *Int J Pharm Pharm Sci.*, 2013, **5**, 627-630.
- [35] M. A Toama, El H. M Fatatry, B. El Falaha, *J Pharm Sci.*, 1978, **67**, 23-26.
- [36] Solangi, A. Rehana, Memon, S. Qayyum, Mallah, Arfana, Memon, Najma, Khuhawar, M. Yar, Bhangar, M. Iqbal, *Pak J Pharm Sci.*, 2011, **24**, 539-544.
- [37] A. Espinosa-Mansilla, A. M. de la Peña, F. Cañada-Cañada, D. G. Gómez, *Anal. Biochem.*, 2005, **347**, 275-286.
- [38] N. Sultana, M. S. Arayne, S. N. Ali, *Am. J. Anal. Chem.*, 2013, **4**, 24-33.
- [39] A. K. Srivastava, R. R. Gaichore, *Anal. Lett.*, 2010, **43**, 1933-1950.
- [40] N. S. Gadhari, B. J. Sanghavi, A. K. Srivastava, *Anal. Chim. Acta.*, 2011, **703**, 31-40.
- [41] B. J. Sanghavi, S. M. Mobin, P. Mathur, G. K. Lahiri, and A. K. Srivastava, *Biosens. Bioelectron.*, 2013, **39**, 124-132.
- [42] N. F. Atta, A. Galal, F. M. Abu-Attia, S. M. Azab, *J. Mater. Chem.*, 2011, **21**, 13015.
- [43] S. Ghosh, M. Narjinary, A. Sen, R. Bandyopadhyay, Somenath Roy, *Sens. Actuators B.*, 2014, **203**, 490-496.
- [44] S.H. Wang, T.C. Chou, C.C. Liu, *Sens. Actuators B.*, 2003, **94**, 343-351
- [45] M. Muti, A. Erdem, A. Caliskan, A. Sinag, T. Yumak, *Colloids Surf. B.*, 2011, **86**, 154-157.
- [46] L. Jiang, S. Gu, Y. Ding, F. Jiang and Z. Zhang, *Nanoscale.*, 2014, **6**, 207
- [47] M. P. Kingsley, P. B. Desai, A. K. Srivastava. *J. Electroanal. Chem.*, 2015, **741**, 71-79
- [48] Ali A. Ensafi, Ali R. Allafchian, B. Rezaei, R. Mohammadzadeh. *Mater Sci Eng C.*, 2013, **33**, 202-208
- [49] Nadir S. E. Osman, Neeta Thapliyal, Wesam S. Alwan, Rajshekhar Karpoormath, Thomas Moyo *J Mater Sci: Mater Electron.*, 2015, **26**, 5097-5105
- [50] S. Ivan and K. Schachl, *Chem. Listy.*, 1999, **93**, 490-499.

- [51] J. Wang, *Analytical Electro Chemistry.*, second ed., Wiley-VCH, New York, 2001.
- [52] Lili Yu et.al., *Food Chem.*, 2015, **176**, 22–26
- [53] Impedance Spectroscopy; Theory, Experiment, and Applications, 2nd ed. , E. Barsoukov, J.R. Macdonald, eds., Wiley Interscience Publications, 2005.
- [54] A. J. Bard, L. R. Faulkner, *Electrochemical Methods Fundamentals and Applications.*, second ed., John Wiley & Sons, New York, 2001.
- [55] Pramod K. Kalambate, Bankim J. Sanghavi, Shashi P. Karna and Ashwini K. Srivastava
Sens. and Act. B, 2015, **213**, 285-294
- [56] X. Zhang, Y. Wei, Y. Ding, *Anal. Chim. Acta.*, 2014, **835**, 29–36.
- [57] L. Fotouhi, M. Alahyari, *Colloids Surf. B.*, 2010, **81**, 110–114.
- [58] A. A. Ensafi, R. Ali. Allafchian, R. Mohammadzadeh, *Anal Sci.*, 2012, **28**, 705-710.
- [59] K. Tyszczyk-Rotko, I. Bęczkowska , M. Wójciak-Kosior, I. Sowa, *Talanta.*,2014, **129**, 384–391.
- [60] A. R. Khaskheli, J. Fischer, J. Barek, V. Vyskocil, Sirajuddina, M. I. Bhanger, *Electrochim. Acta.*, 2013, **101**, 238–242.
- [61] R.T Kachoosangi , G. G Wildgoose , R. G Compton , *Anal. Chim. Acta.*, 2008, **618**, 54–60.

Figure Captions

Fig. 1: SEM images of (A) Graphite; (B) CZF nanoparticles; (C) Graphite – CZF nanocomposite and (D) energy-dispersive X-ray spectrum for CZF nanoparticles.

Fig. 2: Cyclic voltammograms for oxidation of (A) of 5.00×10^{-5} M CIP at; (a) CPE (●●●●) (b) CZF–CME (—) vs. Ag/AgCl (B) of 1.00×10^{-6} M PA at (a) CPE (····) (b) CZF–CME (—) vs. Ag/AgCl; in 0.05M KHP-HCl (pH 3); scan rate 100 mV/s at 25 °C

Fig. 3 Nyquist plots for the EIS measurements for (A) 5.00×10^{-5} M CIP at (a) CPE (●●●●) (b) CZF -CME (◆◆◆) (B) for 1.00×10^{-6} M PA at (a) CPE (●●●●) (b) CZF-CME (◆◆◆) in the frequency range from 10^{-1} to 10^5 Hz , the inset shows an equivalent circuit was used for data fitting.

Fig. 4 Cyclic voltammograms for the oxidation (A) of 5.00×10^{-5} M CIP (B) of 1.00×10^{-6} M PA for scan rate a)50; b)100; c)200; d)300; e) 500; f) 600; g) 700; h) 800; i) 900 mVs^{-1} in 0.05M KHP-HCl (pH 3) at CZF-CME vs. Ag/AgCl at 25 °C.

Fig. 5: AdSDPV curves obtained at CZF -CME for (A) CIP at different concentrations a) 0.02; b) 0.04; c) 0.4; d) 0.8; e) 4.0; f) 6.0; g) 8.0; h) 20.0; i) 40.0; j) 60.0 μM (B) PA at different concentrations a) 0.2; b) 0.4; c) 0.6; d) 0.8; e) 2.0; f) 4.0; g) 6.0; h) 8.0; i) 20.0; j) 40.0 μM : scan rate 100 mVs^{-1} in 0.05M KHP-HCl (pH 3.0): pulse amplitude 60 mV. Inset shows the linearity graph of CIP and PA.

Fig. 6: AdSDPV curves obtained at CZF-CME for **(A)** PA at different concentrations a) 0.4; b) 0.8; c) 2.0; d) 4.0; e) 6.0; f) 8.0; g) 20.0; h) 40.0 μM in the presence of $5.00 \times 10^{-5}\text{M}$ CIP. **(B)** CIP at different concentrations a) 0.02; b) 0.04; c) 0.4; d) 4.0; e) 6.0; f) 8.0; g) 40.0; h) 60.0 μM in the presence of $1.00 \times 10^{-6}\text{M}$ PA in 0.05M KHP –HCl (pH 3.0) scan rate 100 mV/s :pulse amplitude 60 mV. **(C)** simultaneous determination of PA And CIP at different concentrations a) 0.2 & 0.02; b) 0.4 & 0.04; c) 0.8 & 0.06; d) 1.0 & 0.8; e) 1.0 & 2.0; f) 4.0 & 6.0; g) 6.0 & 8.0; h) 8.0 & 20.0; i) 10.0 & 50.0 μM of PA and CIP respectively in 0.05MKHP –HCl (pH 3.0):scan rate 100 mV/s : pulse amplitude 60 mV.

Table Captions:

Table 1: Chronocoulometry of 5.00×10^{-5} M CIP and 1.00×10^{-6} M PA.

Table 2: Analytical parameters for electrochemical determination of CIP and/or PA in 0.05 M KHP –HCl (pH 3) by AdSDPV

Table 3: Comparison of the performances of electrochemical sensors for CIP and PA at CZF-CME in 0.05M KHP-HCl (pH 3.0) by AdSDPV

Table 4: Precision and Bias of assay for standard CIP and PA solution by AdSDPV (n =5)

Table 5: Assay of CIP and /or PA in pharmaceutical preparations (n =5)

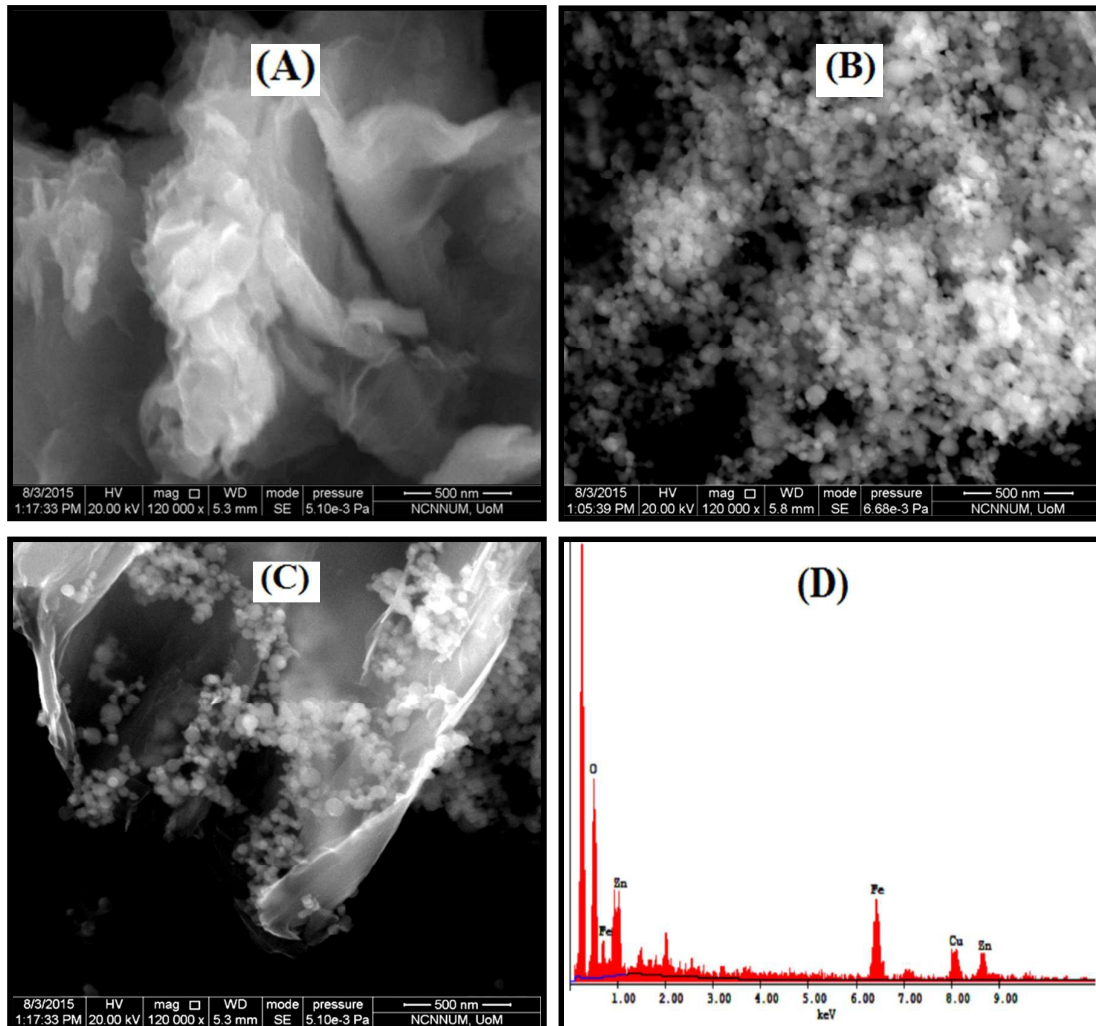


Fig. 1

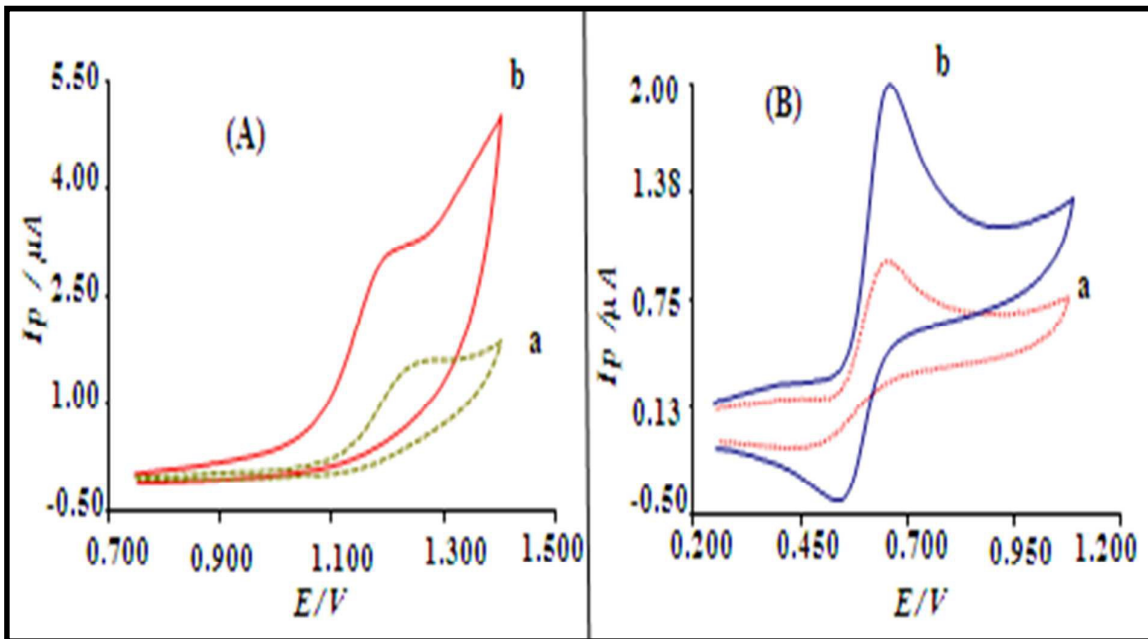


Fig. 2

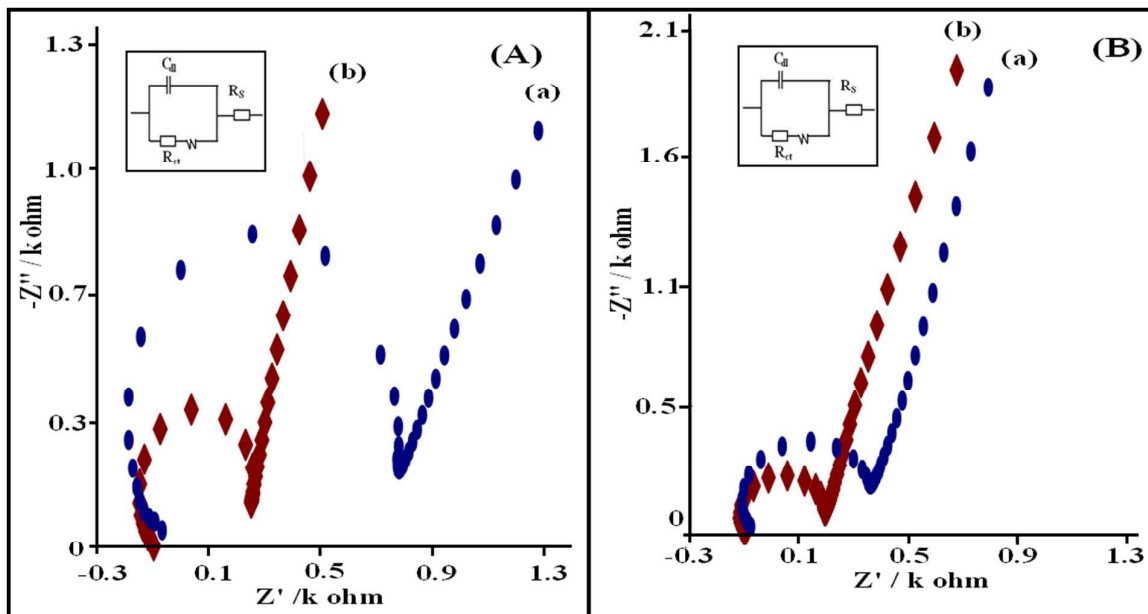


Fig. 3

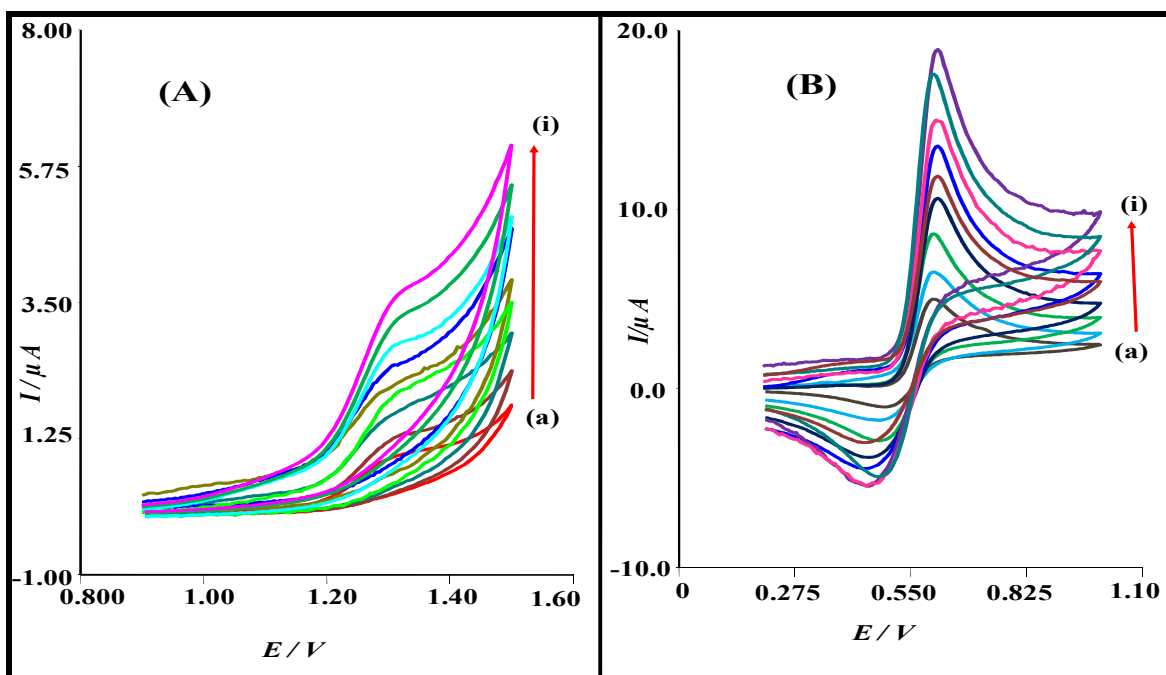


Fig. 4

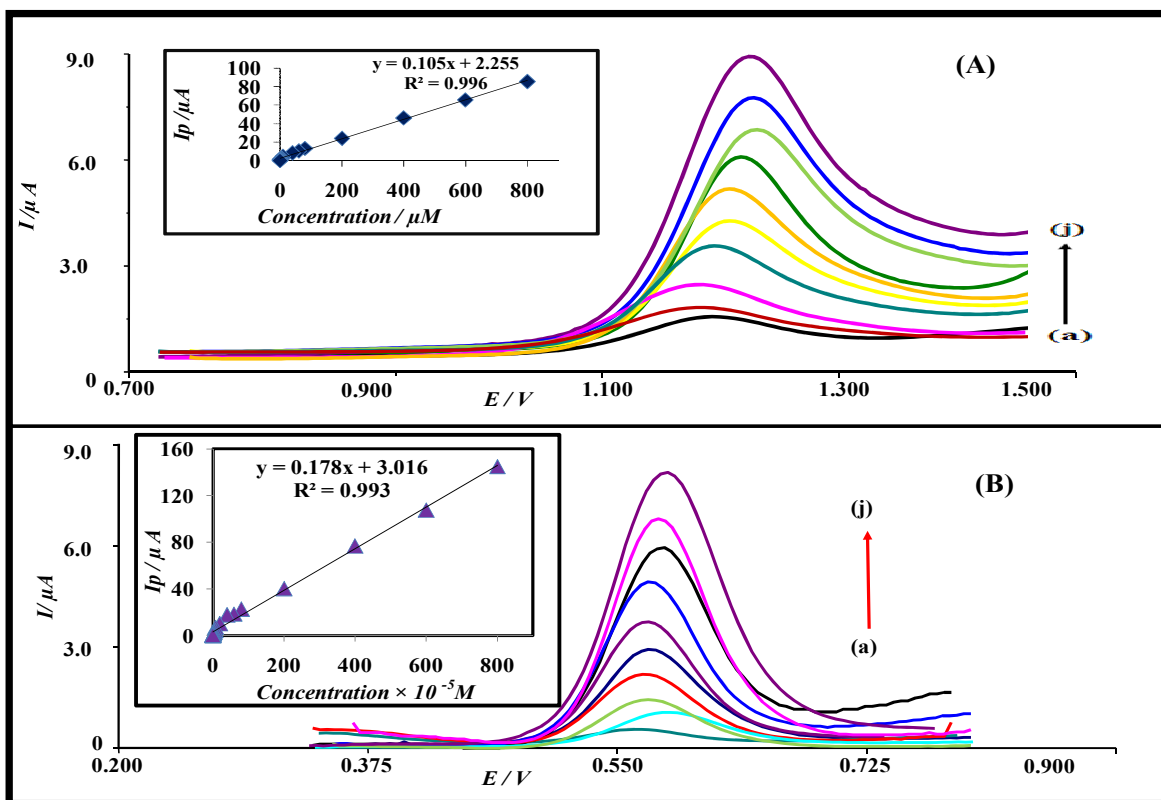


Fig.5

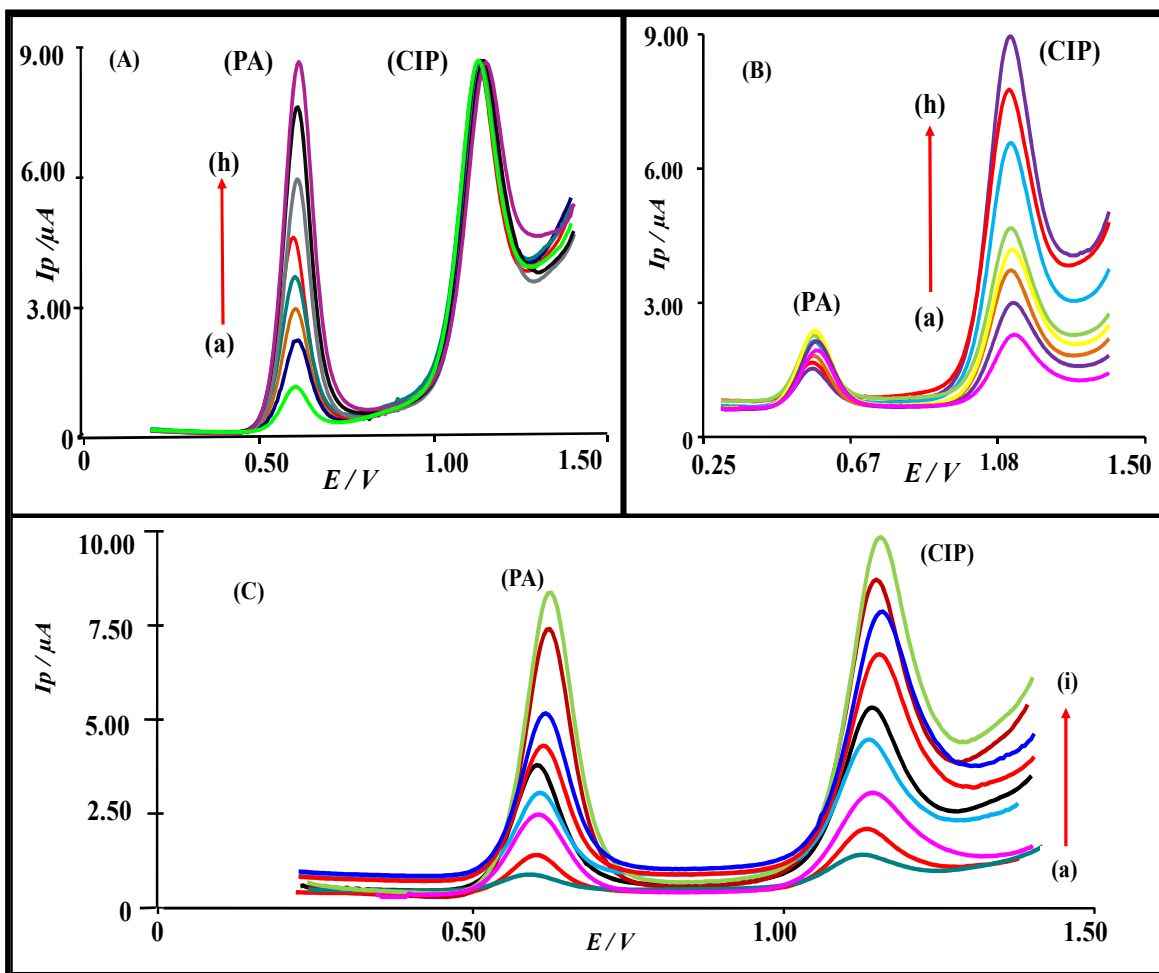


Fig.6

Molecule	Electrode	Slope ($\mu\text{Cs}^{-1/2}$)	Intercept Q_{ads} (μC)	Surface coverage (10^{-9}molcm^{-2})	Diffusion Coefficient (cm^2s^{-1})
CIP	CPE	8.42 ± 1.44	18.17 ± 1.19	4.44	3.32×10^{-10}
	CZF -CME	35.01 ± 0.98	50.00 ± 0.92	5.97	13.71×10^{-10}
PA	CPE	12.94 ± 2.55	28.64 ± 1.84	7.00	7.85×10^{-8}
	CZF -CME	17.45 ± 3.15	82.56 ± 2.68	9.85	15.69×10^{-8}

Table 1

Molecule	LOD	% RSD	LWR	LRE	r
Statistical data for individual molecule					
CIP	$1.38 \times 10^{-9}\text{M}$	2.94	$3.15 \times 10^{-8}\text{M}$ to $6.00 \times 10^{-3}\text{M}$	$I_p (\mu\text{A}) = 0.105 (\mu\text{M})$ + 2.255	0.996
PA	$7.87 \times 10^{-9}\text{M}$	1.46	$4.76 \times 10^{-8}\text{M}$ to $2.63 \times 10^{-4}\text{M}$	$I_p (\mu\text{A}) = 0.178 (10\mu\text{M})$ + 3.016	0.993
Statistical data when CIP concentration increases and PA concentration ($1.00 \times 10^{-6}\text{M}$) remains constant					
CIP	$3.41 \times 10^{-9}\text{M}$	3.74	$9.42 \times 10^{-7}\text{M}$ to $3.98 \times 10^{-3}\text{M}$	$I_p (\mu\text{A}) = 1.265 (\mu\text{M})$ + 3.513	0.984
Statistical data when PA concentration increases and CIP concentration ($5.00 \times 10^{-5}\text{M}$) remains constant					
PA	$2.57 \times 10^{-8}\text{M}$	2.69	$1.66 \times 10^{-7}\text{M}$ to $4.76 \times 10^{-4}\text{M}$	$I_p (\mu\text{A}) = 0.242 (10\mu\text{M})$ + 1.393	0.991
CIP and PA increases in concentration simultaneously					
CIP	$2.58 \times 10^{-9}\text{M}$	1.87	$9.09 \times 10^{-7}\text{M}$ to $4.70 \times 10^{-3}\text{M}$	$I_p (\mu\text{A}) = 0.657 (\mu\text{M})$ + 3.446	0.982
PA	$8.85 \times 10^{-8}\text{M}$	1.76	$1.85 \times 10^{-7}\text{M}$ to $4.76 \times 10^{-4}\text{M}$	$I_p (\mu\text{A}) = 0.248 (10\mu\text{M})$ + 1.118	0.989

Table 2

Molecule	Modified electrode	Detection limit (M)	Linear range (M)	References
Ciprofloxacin	Poly (alizarin red) /graphene composite film	1.00×10^{-8}	4×10^{-8} to 1.2×10^{-4}	56
	Multi-walled nanotube composite film	6.00×10^{-6}	4×10^{-5} to 1.0×10^{-3}	57
	MgFe ₂ O ₄ – MWCNTs	1.00×10^{-8}	1.00×10^{-7} to 1.00×10^{-3}	58
	CZF-CME	1.38×10^{-9}	3.15×10^{-8} to 6.00×10^{-3}	This work
Paracetamol	Boron-doped diamond electrode /Nafion and lead films	1.70×10^{-7}	5.00×10^{-7} to 2.00×10^{-4}	59
	Micro-crystalline natural graphite– polystyrene composite film	3.40×10^{-8}	2.00×10^{-8} to 1.00×10^{-6}	60
	Multiwalled carbon nanotube modified basal plane pyrolytic graphite	4.50×10^{-8}	1.00×10^{-8} to 2.0×10^{-6} & 2.0×10^{-6} to 2.0×10^{-5}	61
	CZF-CME	7.87×10^{-9}	4.76×10^{-8} to 2.63×10^{-4}	This work

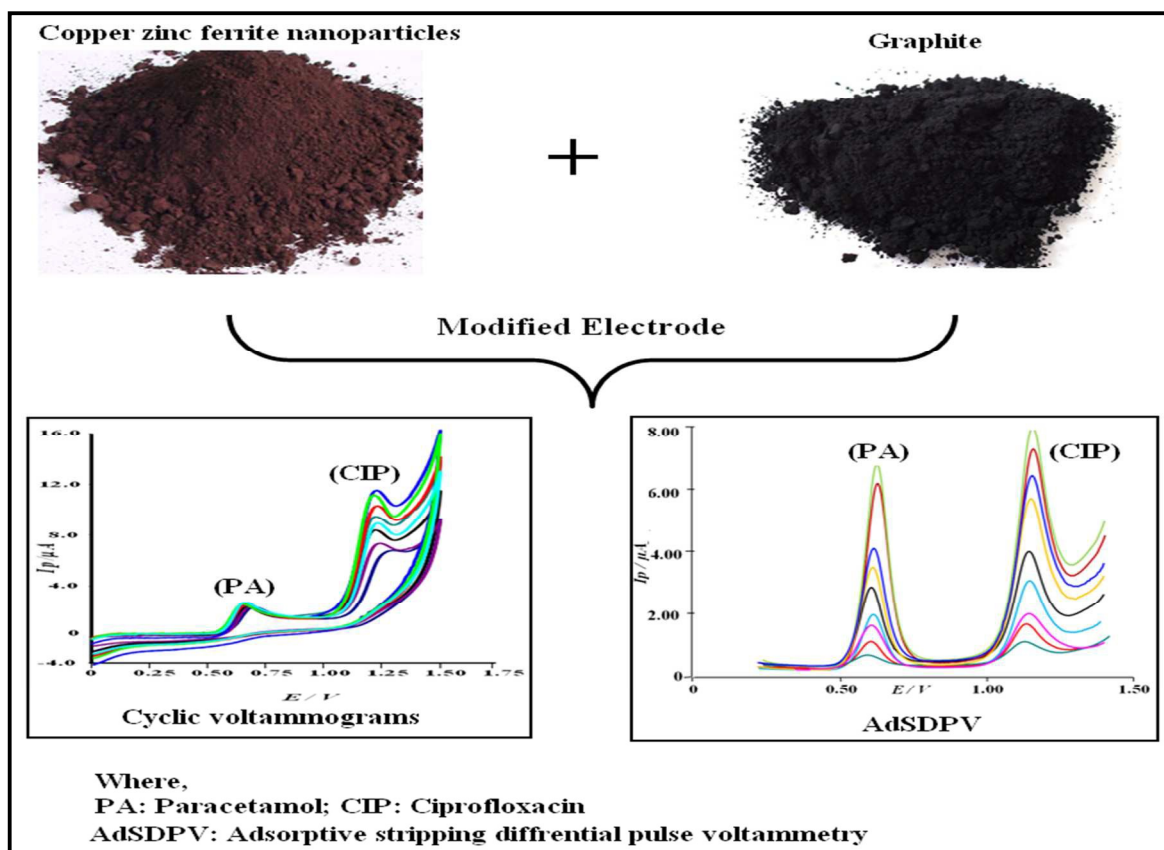
Table 3

Molecule		Concentration taken ($mol L^{-1}$)	Mean concentration found ($mol L^{-1}$)	Bias %	Precision % RSD
CIP	Intra day	1.00×10^{-4}	1.02×10^{-4}	2.00	1.59
	Inter day	1.00×10^{-4}	0.995×10^{-4}	-0.50	1.23
PA	Intra day	1.00×10^{-5}	0.986×10^{-5}	-1.40	2.05
	Inter day	1.00×10^{-5}	1.05×10^{-5}	5.00	1.81

Table 4

Ciprofloxacin			Paracetamol		
Tablet	Amount of drug in the sample (mg)	Amount of drug obtained in the proposed Method (mg) \pm RSD	Tablet	Amount of drug in the sample (mg)	Amount of drug obtained in the proposed method (mg) \pm RSD
Alcipro	500.0	507.7 ± 1.03	Calpol	500.0	506.1 ± 1.83
Cebran	250.0	251.0 ± 2.33	Crocina	500.0	498.7 ± 1.06
Zoxan	250.0	249.3 ± 1.49	—	—	—
—	—	—	Dolo	650.0	651.1 ± 3.14

Table 5



Graphical abstract